PHYSICAL REVIEW B **68**, 085303 (2003)

Effects of internal electrical field on transient absorption in $In_xGa_{1-x}N$ thin layers and quantum wells with different thickness by pump and probe spectroscopy

Kunimichi Omae, Yoichi Kawakami, and Shigeo Fujita
Department of Electronic Science and Engineering, Kyoto University, Kyoto 606-8501, Japan

Yukio Narukawa and Takashi Mukai
Nitride Semiconductor Research Laboratory, Nichia Corporation, 491 Oka, Kaminaka, Anan, Tokushima 774-8601, Japan

(Received 21 October 2002; revised manuscript received 17 March 2003; published 7 August 2003)

The well width dependence of internal electric field effects was investigated using nondegenerate pump and probe spectroscopy at low and room temperature in four types of InGaN-based semiconductors of active layer thicknesses (a) 30 nm (single layer), (b) 10 nm (3 periods), (c) 5 nm (6 periods), and (d) 3 nm (10 periods). For sample (a) and (b) photoinduced absorption was observed due to screening of the internal electric field at low and room temperature. We observed two competing effects, exciton localization and the internal electric field, in sample (c) at low temperature. For sample (d) only photobleaching was observed due to occupation at the localized states. The results show that the field screening effects are more important for increasing well width after carrier generation. Furthermore, the carrier density to observe the photoinduced absorption due to screening the internal electric field is much less than the carrier density for stimulated emission at room temperature.

DOI: 10.1103/PhysRevB.68.085303 PACS number(s): 78.47.+p, 78.67.De, 71.35.−y, 77.65.Ly

I. INTRODUCTION

InGaN-based semiconductors have attracted considerable attention because of their important role in the fabrication of ultraviolet-blue-green light-emitting diodes (LED's) (Refs. 1–3) and laser diodes (LD's).[4,5] Large lattice constant differences between GaN and InN cause two significant effects, fluctuations of In mole fraction due to a miscibility gap,[6–8] and a piezo-electric field due to high strains.[9–11] Fluctuations of In mole fraction induce the localization of excitons that lead to two opposing effects on device performance. One positive effect is the enhancement of internal quantum efficiency of LED's because of the suppression of the pathway to nonradiative recombination centers. Another negative effect is that such localization sometimes results in the increment of lasing threshold due to the limitation of density of states contributing to optical gain. These effects become more significant with increasing the macroscopic In content. Although green LED's with high quantum efficiency have been achieved,[2] stable continuous wave (cw) operation of LD's in the green region has not been reported. In order to understand the optical properties in LD structures, so as to find ways to improve device performance, it is necessary to study a series of samples differing in internal electric field and exciton localization.

It is difficult to separate the internal electric field and exciton localization using conventional photoluminescence (PL) and absorption spectroscopy, because they have almost the same influence on the optical properties, such as large Stokes shifts between absorption and luminescence, a very long PL lifetime, and a strong dependence of PL lifetime on emission energies. Recently, in order to separate these effects, the optical property in cubic InGaN quantum wells excluding the modulation due to internal electric field was reported.[12] Nevertheless, it is important to investigate the optical property in hexagonal InGaN quantum wells, which is usually used for LED and LD. Pump and probe (PP) spectroscopy is a powerful tool for investigating optical properties[13–16] and can separate the two mechanisms. An internal electric field causes photoinduced absorption as well as photobleaching, but exciton localization induces only photobleaching. We have already observed photoinduced absorption in a highly strained GaN film[17] and in an InGaN single epilayer[18] at low temperature. In this paper, the dynamics of photogenerated carriers are investigated in four types of InGaN-based quantum structures using PP spectroscopy at 10 K and room temperature.

II. EXPERIMENTAL

The four types of samples of InGaN-based quantum structures used in this study are composed of, respectively, (a) an $In_{0.1}Ga_{0.9}N$ single layer (30 nm), (b) $In_{0.1}Ga_{0.9}N/GaN$ (10 nm/10 nm) multiple quantum wells (MQW's) with three periods, (c) $In_{0.1}Ga_{0.9}N/GaN$ (5 nm/10 nm) MQW's with six periods, and (d) $In_{0.1}Ga_{0.9}N/GaN$ (3 nm/10 nm) MQWs with ten periods. Although the active layers in each sample differs, the total thickness of the active layers in each sample is 30 nm. All the active layers are sandwiched between GaN layers (0.1 μm) and $Al_{0.1}Ga_{0.9}N/GaN$ (2.5 nm/2.5 nm) superlattices with 100 periods. All layers are grown on GaN buffer layers and sapphire substrates under an undoped condition.

The temporal behavior of differential absorption was measured by PP spectroscopy using a dual photodiode array in conjunction with a 25 cm monochromator. The experimental setup for PP spectroscopy was depicted in Ref. 19. The white light used for the probe beam was generated by focusing part of the output beam from the regenerative amplifier on a D_2O cell. The white light was always monitored using a dual photo-diode array. And the all spectra were divided by the spectra of the monitered white light to exclude the affect of white light fluctuations. The pump beam was created using an optical parametric amplifier laser with its wavelength ad-

 ©2003 The American Physical Society

justed to 370 nm in order to achieve selective excitation in the InGaN active layers. The pulse widths of both the pump and probe beams were 150 fs. The optical delay time of the probe beam with respect to the pump beam was tuned by changing the position of the retroreflector, which could be controlled by the pulse stage. In order to allow detection of a probe beam with a spatially uniform carrier distribution in the sample, the focus size of the pump beam (500 μm in diameter) was set so as to be much larger than the probe beam (100 μm in diameter). Furthermore, the probe beam was polarized perpendicular to the pump beam, and the transmitted probe beam polarized in this direction was detected to avoid detecting the scattered component of the pump beam.

III. RESULTS AND DISCUSSION

The dynamic behavior of dense carriers was characterized by the measurement of ΔOD by PP spectroscopy for each sample at two temperatures, 10 K and room temperature. ΔOD is expressed by the following equation:

$$\Delta OD = \log_{10}\left(\frac{T}{T+\Delta T}\right) = \Delta \alpha d \times 0.434,$$

where T and $T+\Delta T$ are the probe beam intensities in the absence and presence of the pump beam, respectively. $\Delta\alpha$ is the photoinduced change of the absorption coefficient and d is the thickness of the absorbing layers. Therefore, for $\Delta OD<0$ absorption decreases due to bleaching, and for $\Delta OD>0$ absorption increases due to the effect of the photoinduced enhancement.

Figure 1 shows the variation of the ΔOD spectra at 10 K as a function of time after pumping at 370 nm (3.350 eV) under the relatively strong photoexcitation of $I_{ex} = 800\ \mu J/cm^2$, for each of the four samples. The carrier density just after the photoexcitation is estimated about $1.2 \times 10^{20}\ cm^{-3}$.[20] OD spectra taken under weak photoexcitation are shown as references. PL spectra are also shown, under both the same and weak excitation conditions, except for sample (c). For sample (c) the PL spectrum under the weak excitation condition was located at about 2.7 eV and was very different from the ΔOD and PL spectra under the strong excitation condition, and hence is not shown. Stimulated emission can be seen at about 3.1 eV in all samples under this strong excitation condition. Therefore, the macroscopic In content seems to be almost the same in each sample. The stimulated emission was confirmed in all samples by time resolved photoluminescence (TRPL). Since the PL lifetime of stimulated emission was much shorter than that of spontaneous emission, we can easily confirm the stimulated emission using TRPL.[21–23] The threshold carrier density for stimulated emission was estimated on the order of $10^{18}\ cm^{-3}$ at low temperature. The redshift of the PL peak was observed for strong excitation in the case of samples (a) and (b). It is thought that the internal electric field was screened by photogenerated carrier even under the weak excitation condition. The carrier recombination will not occur in sample (a) and (b) when the electrons and holes are perfectly separated by the internal electric field without screening. The redshift of stimulated emission has been commonly observed from nitride-based materials by many researchers.[24–27] The possible origin of redshift of the PL peak for strong excitation is the many body effects of carriers.

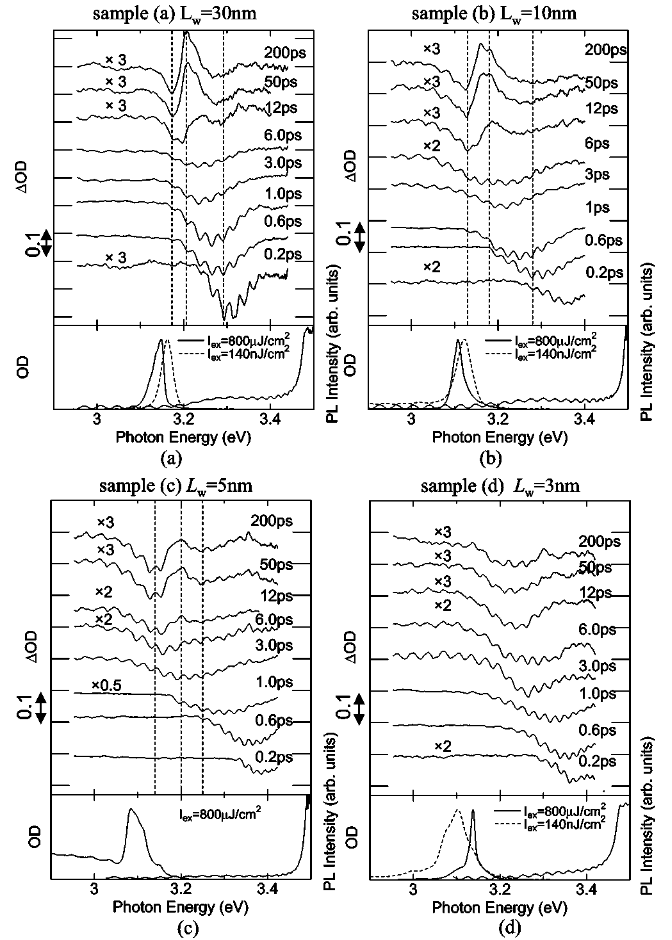

FIG. 1. Variation of ΔOD spectra for each of the four samples as a function of time after pumping at 370 nm (3.350 eV) under $I_{ex} = 800\ \mu J/cm^2$ at 10 K. The OD spectra taken under weak photoexcitation and the PL spectra under the same and weak excitation conditions are shown at the bottom of each plot.

In all the samples, the photogenerated carriers rapidly reached the bottom level in the active layer after only a few ps. In samples (a) and (b) positive peaks are observed after about 15 ps, at 3.21 eV for sample (a) and 3.17 eV for sample (b). The stimulated emission peak is located about 70 meV lower in energy than the photoinduced absorption peak in each sample, suggesting that the stimulated emission occurs at localization states. In samples (c) and (d), only negative signals were obtained over the whole time and energy range. After 50 ps the shape of the spectra in sample (c) are different from those of sample (d). The spectra in sample (d) are merely broadened from 3.1 to 3.35 eV, while the spectra in sample (c) tend toward the same structure as samples (a) and (b) at about 3.2 eV, though the signal does not become positive. The mechanism of photoinduced enhancement observed in samples (a) and (b) is probably the same as

observed in a GaN epilayer, where screening of the internal electric field takes place.[18] In sample (d), however, only photobleaching is observed, due the localization states of the excitons being occupied. In sample (c), the overlapping of both effects is clearly observed. A band filling effect results in simple photobleaching spectra similar to those of sample (d). On the other hand, screening of the internal electric field induces positive signals sandwiched between the two negative signals as in samples (a) and (b). When both effects are observed at the same time, the signal, which is turned slightly in a positive direction, is observed between two strong negative signals, as seen in the sample (c) spectra at $t=50$ and 200 ps. In samples (a) and (b) the screening of the internal electric field has a dominant effect on optical transitions after carrier generation. The internal electric field reduces the oscillator strength of optical transition due to Stark effects and Frantz-Keldysh effects. When the photogenerated carriers screen the internal electric field, excitonic absorption is restored. As a result, photoinduced enhancement of the absorption coefficient is observed. The internal electric field strength due to piezoelectric polarization was calculated to be 0.45–1.6 MV/cm using the scattered value of the piezoelectric constants.[28,29] In sample (d) exciton localization has a dominant effect on optical transitions. The density of localized levels is so small that the DOS is easily occupied by the photo-generated carriers. As a result, the broad negative signals of ΔOD are observed. Piezoelectric field dominates over inhomogeneity in samples with layer thickness more than the exciton Bohr radius (3.4 nm). Our result was consistent with the previous works.[30,31] Physical mechanism was also stated in Refs. 30 and 31.

We next consider the ΔOD spectra under the weak excitation condition, to determine whether the difference in ΔOD after 50 ps is dependent on the carrier density due to the difference in the threshold carrier density for stimulated emission. The lifetime of simulated emission is much shorter than that of spontaneous emission, so the carrier density after 50 ps is almost the same as the threshold carrier density for stimulated emission in each sample. Figure 2 shows the ΔOD spectra for each sample under the weak excitation condition. The excitation density is about $I_{ex}=8$ μJ/cm^2 in samples (a) and (b), and about $I_{ex}=80$ μJ/cm^2 in samples (c) and (d). The carrier density just after photoexcitation was estimated about 1.2×10^{19} and 1.2×10^{18} cm^{-3} under $I_{ex}=80$ μJ/cm^2 and $I_{ex}=8$ μJ/cm^2, respectively.[20] For samples (c) and (d) the ΔOD signal level was reduced compared to that under $I_{ex}=800$ μJ/cm^2, and no clear data could be obtained for $I_{ex}=8$ μJ/cm^2 because of both the detection limit and interference effect. Moreover, the broadness of the spectra, due probably to the potential fluctuation, leads to difficulties in detection under smaller photogenerated carriers. Nevertheless, positive signals are observed only in samples (a) and (b), over the whole time range. As mentioned above, the internal electric field has a dominant effect on optical transitions in samples (a) and (b). The difference in the threshold carrier density is not significant for these ΔOD spectra at low temperature.

The temporal behavior of the ΔOD spectra under strong excitation at room temperature is shown in Fig. 3. All the

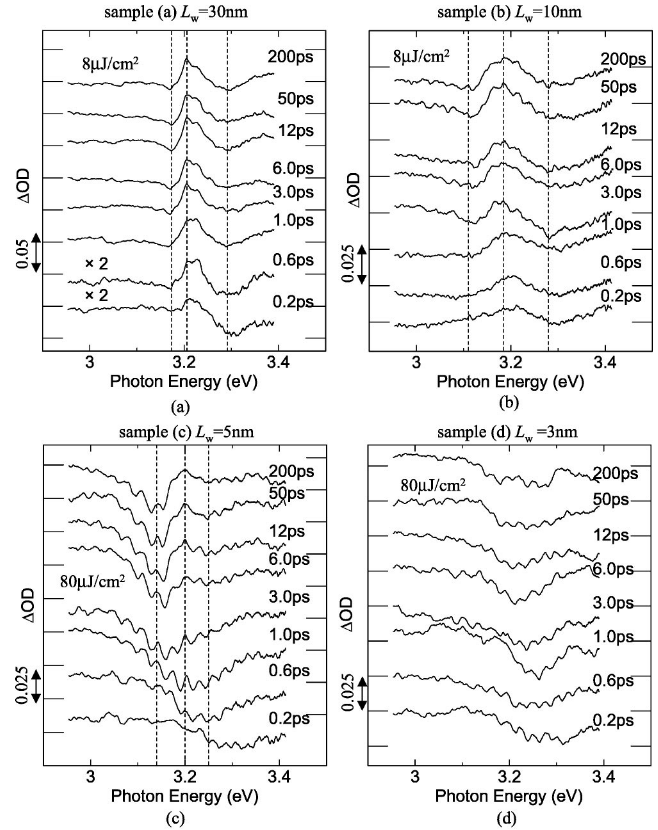

FIG. 2. Variation of ΔOD spectra as a function of time under weak excitation at 10 K. The excitation density is about $I_{ex}=8$ μJ/cm^2 for samples (a) and (b) and about $I_{ex}=80$ μJ/cm^2 for samples (c) and (d).

ΔOD spectra at room temperature for samples (a) and (b) as well as samples (c) and (d) have only broad negative signals in contrast to the low temperature case illustrated in Fig. 1. This is probably due to an increase in the threshold carrier density for stimulated emission. The threshold carrier density for stimulated emission at room temperature is so high that the photogenerated carrier density does not decrease sufficiently within the time range of our experiment. It is difficult to estimate the carrier density just after photoexcitation at room temperature, because with piezoelectric field in the barrier GaN layer, the GaN barrier layer absorption tail extends to 370 nm. But it is thought the order of carrier density can be estimated. The carrier density under 800 μJ/cm^{-2} was on the order of 10^{20} cm^{-3}. The threshold carrier density for stimulated emission was more than the order of 10^{19} cm^{-3}. This means that the saturation of the absorption is much larger than the photoinduced absorption at high carrier density. Similar behavior was also observed at low temperature for samples (a) and (b) within 15 ps. The threshold carrier density at low temperature, however, is low enough that the photogenerated carrier density rapidly decreases to the carrier density where the saturation of the absorption is ignored.

In order to confirm the effect of the threshold carrier density, PP spectroscopy under the weak excitation condition was performed at room temperature and illustrated in Fig. 4. In samples (a) and (b) photoinduced absorption was ob-

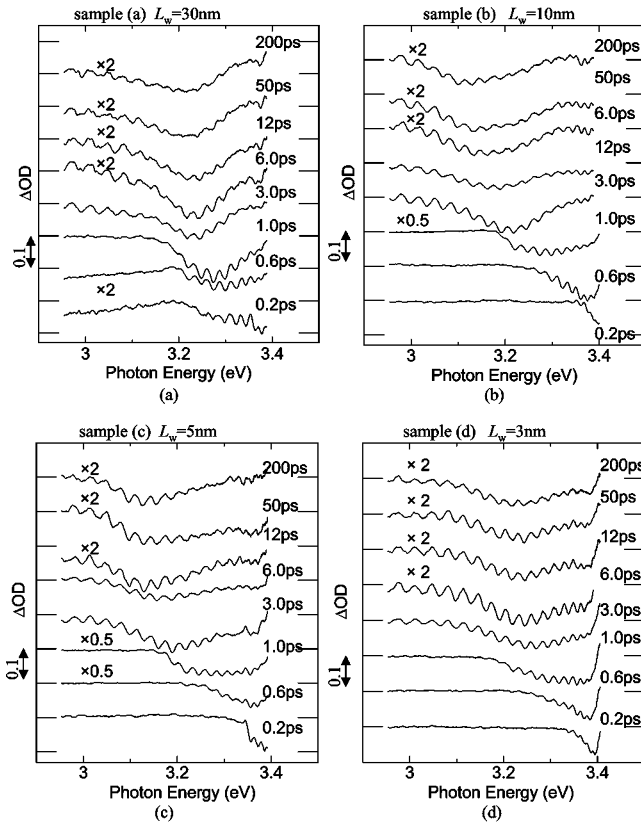

FIG. 3. Variation of ΔOD spectra as a function of time after pumping under $I_{ex} = 800\ \mu J/cm^2$ at room temperature.

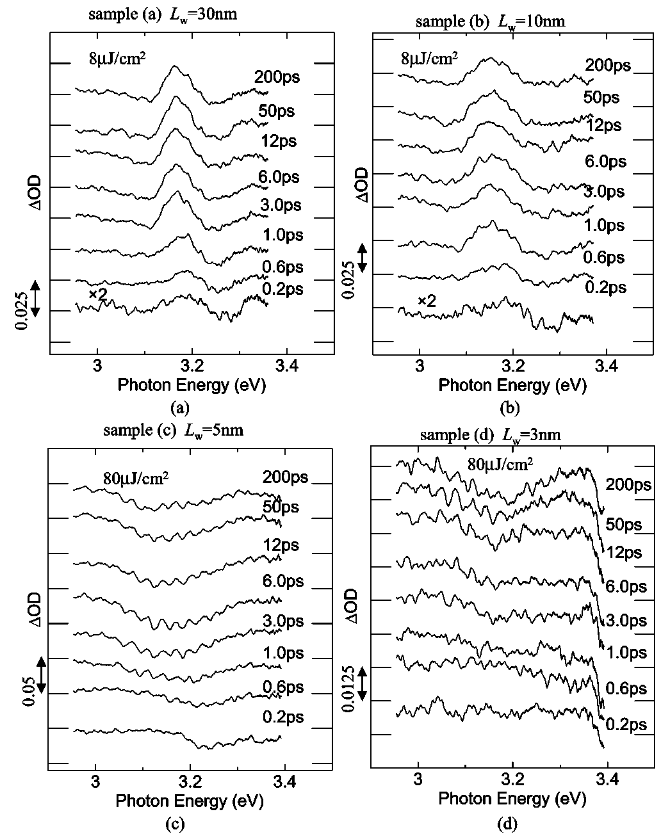

FIG. 4. The variation of ΔOD spectra as a function of time after pumping under weak excitation at room temperature. The excitation density is about $I_{ex} = 8\ \mu J/cm^2$ for samples (a) and (b), and about $I_{ex} = 80\ \mu J/cm^2$ for samples (c) and (d).

served just after photopumping. Only negative signals were obtained in samples (c) and (d) over the whole time range. This behavior is almost the same as that at low temperature under the weak excitation condition. However, the ΔOD spectra for sample (c) at room temperature does not have the structure seen at low temperature. This is because the internal electric field in sample (c), which is relatively low even at low temperature, is screened by intrinsic carriers originating from unintentional doping by impurities or defects activated by thermal energy. These results suggest that the carrier density to observe the photoinduced absorption due to screening the piezoelectric field is much less than that for simulated emission at room temperatures.

IV. CONCLUSION

From our investigation of the well width dependence of the internal electric field on optical transition in different types of InGaN-based semiconductors at low and room temperature, it was found that the screening of internal electric fields are more important than exciton localization after carrier generation as the thickness of a single active layer is increased. In sample (c) the two competing effects of exciton localization and the internal electric field could be observed at low temperature. However, at room temperature only the exciton localization effect was observed in sample (c). The electric field in sample (c) is easily screened by unintentional doping by impurities and defects activated by thermal energy. Photoinduced absorption was observed under the weak excitation condition in samples (a) and (b) at both low and room temperature. At room temperature, the carrier density to observe the photoinduced absorption due to screening the internal electric field is much less than that for stimulated emission, because the photoinduced absorption was not observed under strong excitation condition.

ACKNOWLEDGMENT

Part of this study was carried out using the facility at the Venture Business Laboratory in Kyoto University (KU-VBL).

[1] S. Nakamura, M. Senoh, N. Iwasa, and S. Nagahama, Jpn. J. Appl. Phys., Part 2 **34**, L797 (1995).

[2] S. Nakamura, M. Senoh, N. Iwasa, S. Nagahama, T. Yamada, and T. Mukai, Jpn. J. Appl. Phys., Part 2 **34**, L1332 (1995).

[3] T. Mukai, M. Yamada, and S. Nakamura, Jpn. J. Appl. Phys., Part 2 **37**, L1358 (1998).

[4] S. Nagahama, T. Yanamoto, M. Sano, and T. Mukai, Jpn. J. Appl. Phys., Part 2 **40**, L788 (2001).
[5] S. Nagahama, T. Yanamoto, M. Sano, and T. Mukai, Appl. Phys. Lett. **79**, 1948 (2001).
[6] T. Matsuoka, Appl. Phys. Lett. **71**, 105 (1997).
[7] Y. Narukawa, Y. Kawakami, M. Funato, Sz. Fujita, Sg. Fujita, and S. Nakamura, Appl. Phys. Lett. **70**, 868 (1997).
[8] S. Chichibu, K. Wada, and S. Nakamura, Appl. Phys. Lett. **71**, 2346 (1997).
[9] T. Takeuchi, S. Sota, M. Katsuragawa, M. Komori, H. Takeuchi, H. Amano, and I. Akasaki, Jpn. J. Appl. Phys., Part 2 **36**, L382 (1997).
[10] C. Wetzel, T. Takeuchi, H. Amano, and I. Akasaki, Phys. Rev. B **62**, R13 302 (2000).
[11] T. Kuroda, A. Tackeuchi, and T. Sota, Appl. Phys. Lett. **76**, 3753 (2000).
[12] S.F. Chichibu, M. Sugiyama, T. Onuma, T. Kitamura, H. Nakanishi, T. Kuroda, A. Tackeuchi, T. Sota, Y. Ishida, and H. Okumura, Appl. Phys. Lett. **79**, 4319 (2001).
[13] A. Satake, Y. Masumoto, T. Miyajima, T. Asatsuma, and M. Ikeda, Phys. Rev. B **60**, 16 660 (1999).
[14] C.K. Choi, Y.H. Kwon, J.S. Krasinski, G.H. Park, G. Setlur, J.J. Song, and Y.C. Chang, Phys. Rev. B **63**, 115315 (2001).
[15] C.K. Sun, Y.-L. Huang, S. Keller, U.K. Mishra, and S.P. Denbaars, Phys. Rev. B **59**, 13 535 (1999).
[16] A. Shikanai, T. Deguchi, T. Sota, T. Kuroda, A. Tackeuchi, S. Chichibu, and S. Nakamura, Appl. Phys. Lett. **76**, 454 (2000).
[17] K. Omae, Y. Kawakami, Sg. Fujita, M. Yamada, Y. Narukawa, and T. Mukai, Phys. Rev. B **65**, 073308 (2002).
[18] K. Omae, Y. Kawakami, Y. Narukawa, Y. Watanabe, T. Mukai, and Sg. Fujita, Phys. Status Solidi A **190**, 93 (2002).
[19] Y. Kawakami, K. Omae, A. Kaneta, K. Okamoto, T. Izumi, S. Saijou, K. Inoue, Y. Narukawa, T. Mukai, and Sg. Fujita, Phys. Status Solidi A **183**, 41 (2001).
[20] The carrier density just after photoexcitation was estimated from the absorption coefficient (about 1×10^5 cm^{-1}), the active layer thickness (30 nm) and the photoexcitation density.
[21] Y. Narukawa, Y. Kawakami, Sg. Fujita, and S. Nakamura, Phys. Status Solidi A **176**, 39 (1999).
[22] X.Q. Shen, M. Shimizu, H. Okumura, and F. Sasaki, Appl. Phys. Lett. **79**, 1599 (2001).
[23] C.K. Choi, B.D. Little, Y.H. Kwon, J.B. Lam, J.J. Song, Y.C. Chang, S. Keller, U.K. Mishra, and S.P. DenBaars, Phys. Rev. B **63**, 195302 (2001).
[24] H. Amano, T. Tanaka, Y. Kunii, K. Kato, S.T. Kim, and I. Akasaki, Appl. Phys. Lett. **64**, 1377 (1994).
[25] X.H. Yang, T.J. Schmidt, W. Shan, J.J. Song, and B. Goldenberg, Appl. Phys. Lett. **66**, 1 (1995).
[26] M.A. Khan, C.J. Sun, J.W. Yang, Q. Chen, B.W. Lim, M.Z. Anwar, A. Osinsky, and H. Temkin, Appl. Phys. Lett. **69**, 2418 (1996).
[27] J. Wu, H. Yaguchi, K. Onabe, and Y. Shiraki, Appl. Phys. Lett. **73**, 1 (1998).
[28] S.F. Chichibu, T. Sota, K. Wada, O. Brandt, K.H. Ploog, S.P. Denbaars, and S. Nakamura, Phys. Status Solidi A **183**, 91 (2001).
[29] F. Bernardini, V. Fiorentini, and D. Vanderbilt, Phys. Rev. B **56**, R10 024 (1997).
[30] S.F. Chichibu, A.C. Abare, M.S. Minsky, S. Keller, S.B. Fleischer, J.E. Bowers, E. Hu, U.K. Mishra, L.A. Coldren, S.P. DenBaars, and T. Sota, Appl. Phys. Lett. **73**, 2006 (1998).
[31] E. Berkowicz, D. Gershoni, G. Bahir, E. Lakin, D. Shilo, E. Zolotoyabko, A.C. Abare, S.P. Denbaars, and L.A. Coldren, Phys. Rev. B **61**, 10 994 (2000).